Appendix 2: Apparent versus true GH axial rotation with the scapular lateral axis defined by the acromial angle (posterolateral acromion)

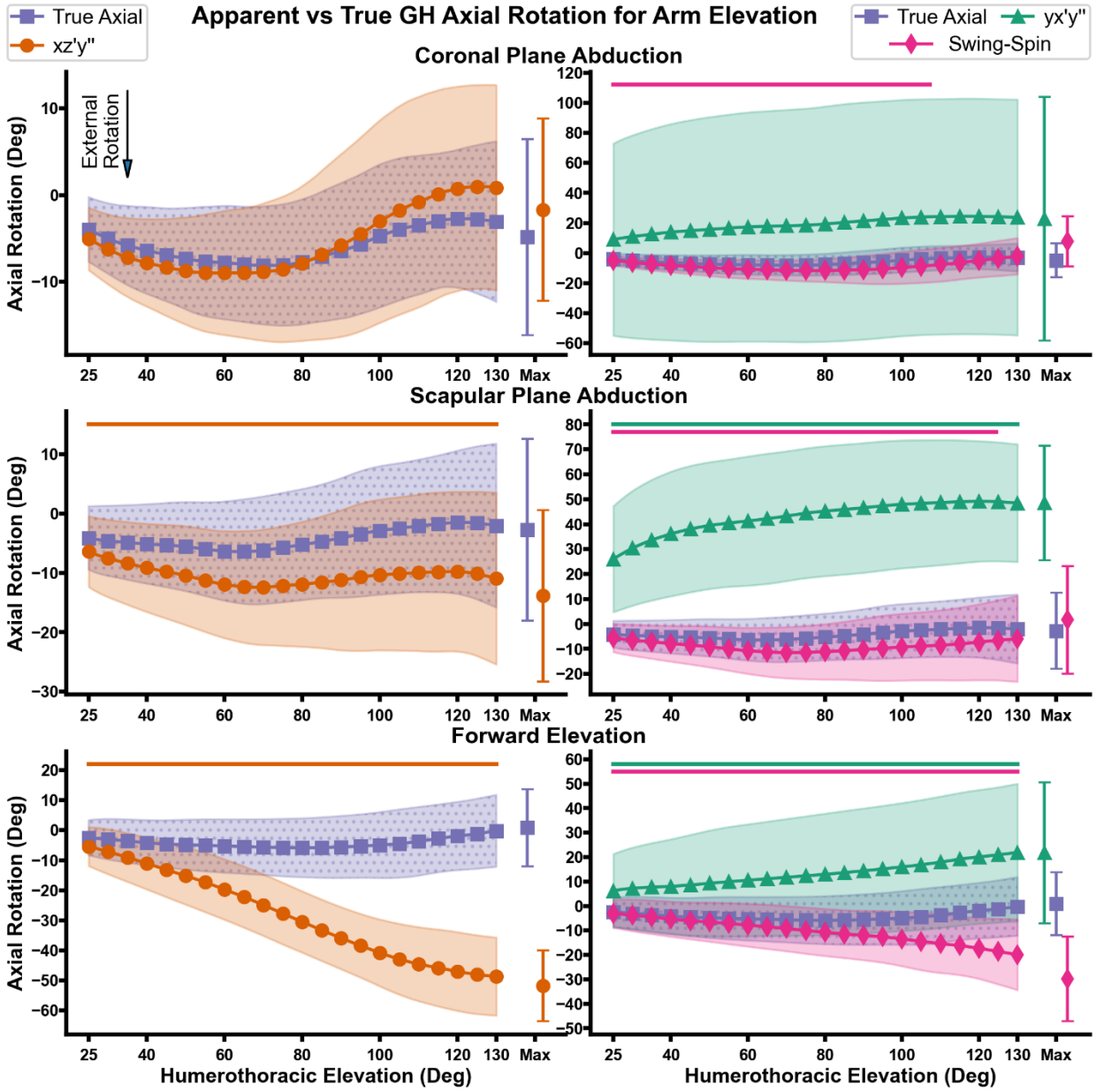

Fig A2a: Comparison of xz'y'' (left), yx'y'' (right), and swing-spin (right) apparent GH axial rotation versus true GH axial rotation for CA (top), SA (middle), and FE (bottom) when the scapula lateral direction is defined by the acromial angle (posterolateral acromion). The singular data point indicates axial rotation at maximum HT elevation (differs by subject). The errors bars around the singular data point and the shaded regions indicate ±1 standard deviation. The solid lines (orange for xz'y'', green for yx'y'', and magenta for swing-spin) at the top of each plot indicate regions where a SPM1D non-parametric paired t-test found significant differences between apparent and true axial rotation.

Appendix 2: Apparent versus true GH axial rotation with the scapular lateral axis defined by the acromial angle (posterolateral acromion)

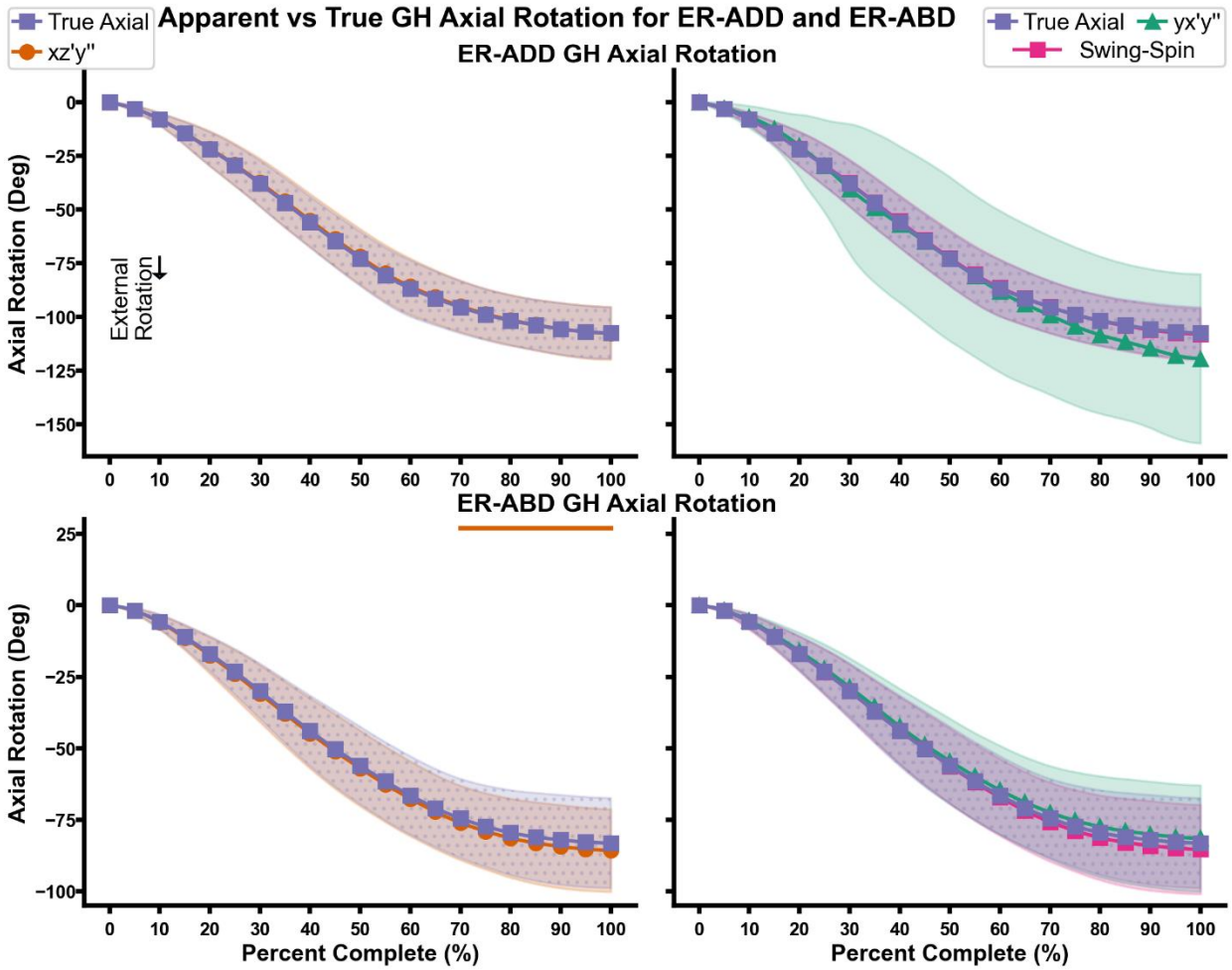

Fig A2b: Comparison of xz'y'' (left), yx'y'' (right), and swing-spin (right) GH apparent axial rotation versus true GH axial rotation for ER-ADD (top) and ER-ABD (bottom) when the scapula lateral direction is defined by the acromial angle (posterolateral acromion). Trials were interpolated at 0.25% increments between the start (0%) of the motion and maximum external rotation (100%). The shaded regions indicate ±1 standard deviation. The solid lines (orange for xz'y'', green for yx'y'', and magenta for swing-spin) at the top of each plot indicate regions where a SPM1D non-parametric paired t-test found significant differences between apparent and true axial rotation.